Electronic Supplementary Material (ESI) for Nanoscale

Supplemental Material

Low activation energy for the crystallization of amorphous silicon nanoparticles

Thomas Lopez, Lorenzo Mangolini

Mechanical Engineering Department, Materials Science and Engineering Program

University of California, Riverside CA 92521

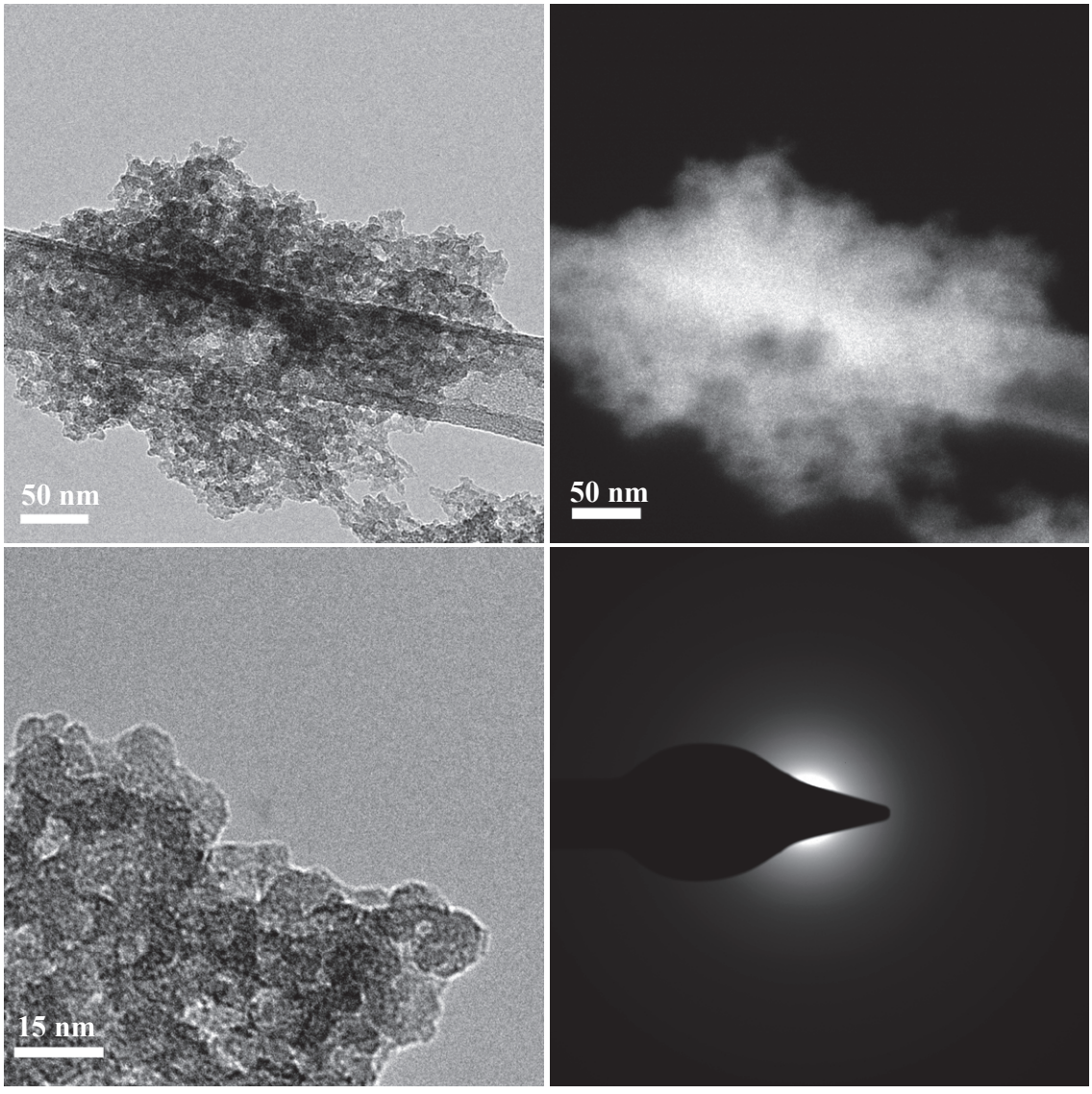

Figure S1. (a) TEM micrograph of amorphous silicon particles produced under the conditions of 'sample A' (see Table 1) without any in-flight annealing. (b) Dark field micrograph of figure (a). (c) higher magnification micrograph for the sample, and (d) corresponding selected area diffraction (SAD) pattern.

A lower magnification image was used to generate the diffraction pattern, so that a large number of particles interacts with the electron beam. The combination of weak contrast in the dark field image, lack of fringes in the higher magnification image, and weak pattern in the SAD leads to conclude that the particle have an amorphous structure.

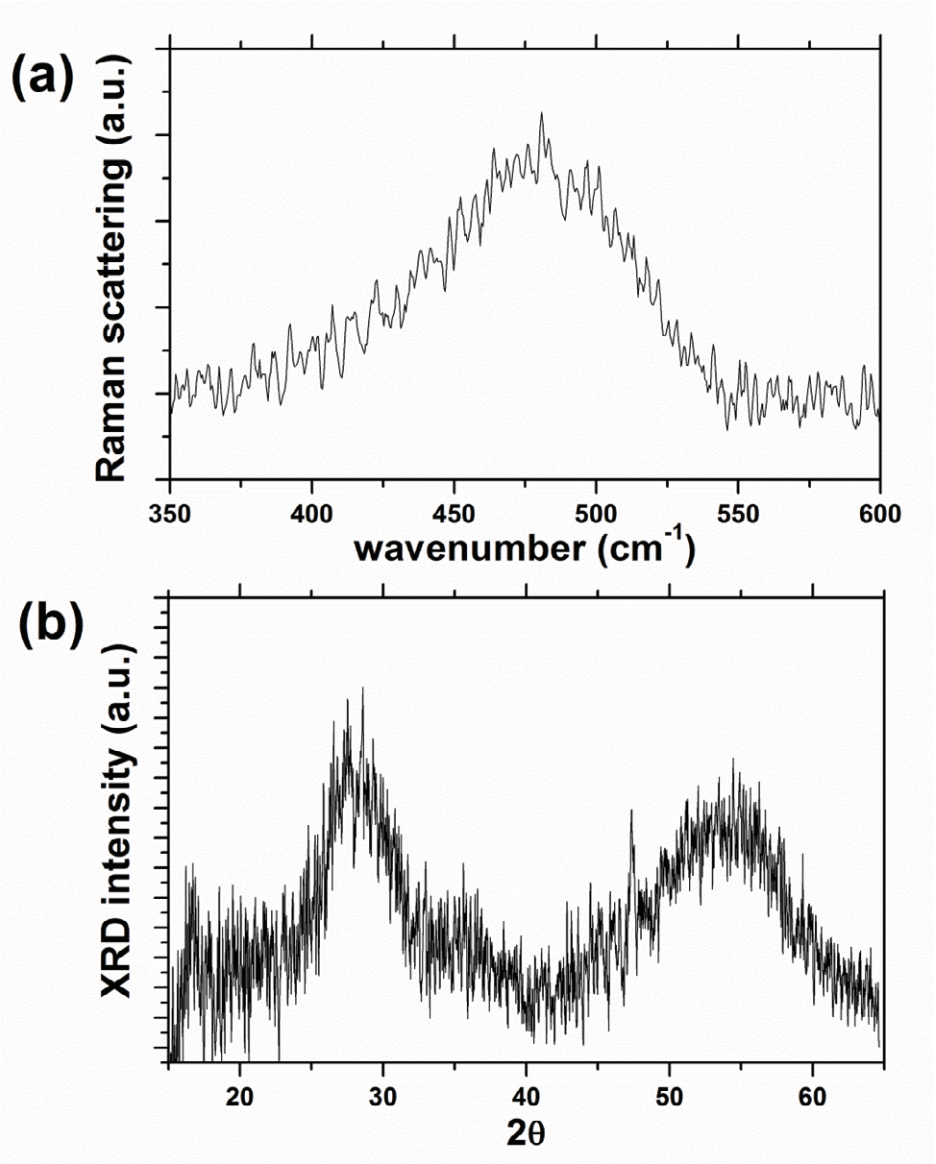

Figure S2. (a) Raman scattering from samples produced under the conditions of 'sample A' (see table 1) without any in-flight annealing. (b) XRD for the same sample of (a). Both Raman and XRD data support the conclusion that the particles have an amorphous structure.

Summary of expression for the RWL, Paillard and Faraci peak profiles:

$$\text{RWL:} \qquad I(\omega) = A \cdot \int_0^1 \frac{\exp\left(-q^2 L^2 / 4\right) q^2}{[\omega - \omega(q)]^2 + \left(\Gamma_c / 2\right)^2} dq$$

Where $\omega(q) = \omega_c \cdot \left(1 - 0.23 \cdot q^2\right)$, q is the non-dimensional wavenumber, ω is frequency (in units of cm^{-1}), ω_c = 521 cm^{-1}, L is the non-dimensional nanoparticle size and is equal to d/a_0, with d = particle size in nanometers, and a_0 is the lattice constant (0.543 nm for Si). Γ_c is the natural line with for Si at room temperature (4.6 cm^{-1}). A is a scaling factor and a fitting parameter, together with the particle size.

$$\text{PAILLARD:} \qquad I(\omega) = A \cdot \int_{-0.5}^{0.5} \frac{\sin^2(\pi q L) / \left(1 - q^2 L^2\right)}{[\omega - \omega(q)]^2 + \left(\Gamma_c / 2\right)^2} dq$$

Where $\omega(q) = \sqrt{\omega_c^2 - 126100 \cdot q^2 / |q| + 0.53}$, q is the non-dimensional wavenumber, ω is frequency (in units of cm^{-1}), ω_c = 521 cm^{-1}, L is the non-dimensional nanoparticle size and is equal to d/a_0, with d = particle size in nanometers, and a_0 is the lattice constant (0.543 nm for Si). Γ_c is the natural line with for Si at room temperature (4.6 cm^{-1}). A is a scaling factor and a fitting parameter, together with the particle size.

$$\text{FARACI:} \qquad I(\omega) = A \cdot \int_{2\cdot\pi-1}^{2\cdot\pi+1} \frac{\sin\left(q/2\right) / q \cdot \left(4 \cdot \pi^2 - q^2\right)}{[\omega - \omega(q)]^2 + \left(\Gamma_c / 2\right)^2} dq$$

Where $\omega(q) = \sqrt{171400 + 100000 \cdot \cos\left(q \cdot L / 4\right)}$, q is the non-dimensional wavenumber, ω is frequency (in units of cm^{-1}), ω_c = 521 cm^{-1}, L is the non-dimensional nanoparticle size and is equal to d/a_0, with d = particle size in nanometers, and a_0 is the lattice constant (0.543 nm for Si). Γ_c is the natural line with for Si at room temperature (4.6 cm^{-1}). A is a scaling factor and a fitting parameter, together with the particle size.

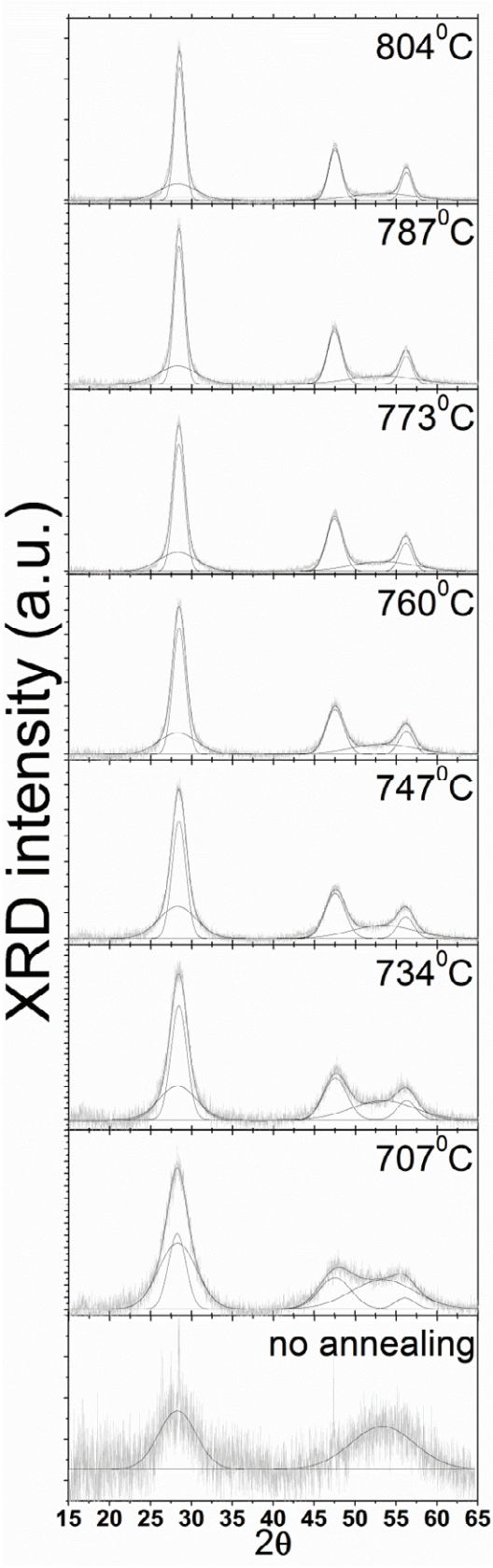

Figure S3. Fitting of XRD data for the determination of the crystalline fraction. A five-peaks procedure is used, with the center and width of the two peaks due to the amorphous phase determined using the XRD data for the sample that has not been annealed (see graph labeled as 'no annealing'). The five peaks fit is then performed by holding constant the position and width for the two peaks corresponding to the amorphous contribution, while fitting their amplitude together with that of the peaks arising from the crystalline structure. The crystalline fraction is quantified by calculating the ratio between the area under the three sharper peaks due to the crystalline structure (from the [111], [220] and [311] lattice planes) over the total area (area from the crystalline peaks summed with the area from the two amorphous features). The in-flight annealing temperatures are clearly labeled on the graphs.

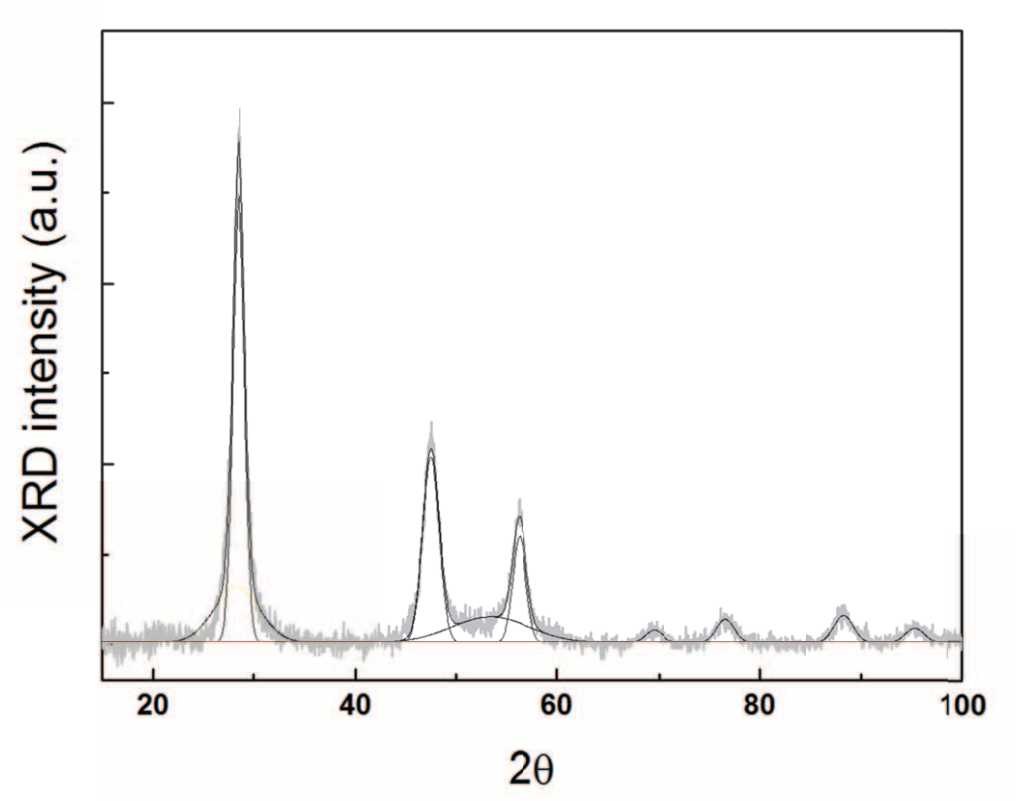

plane	2θ	FWHM
[111]	28.47895	1.4415
[220]	47.48861	1.90036
[311]	56.22458	1.64053
[400]	69.48807	2.01858
[331]	76.58974	2.06393
[442]	88.26317	2.22249
[511]	95.23489	2.17635

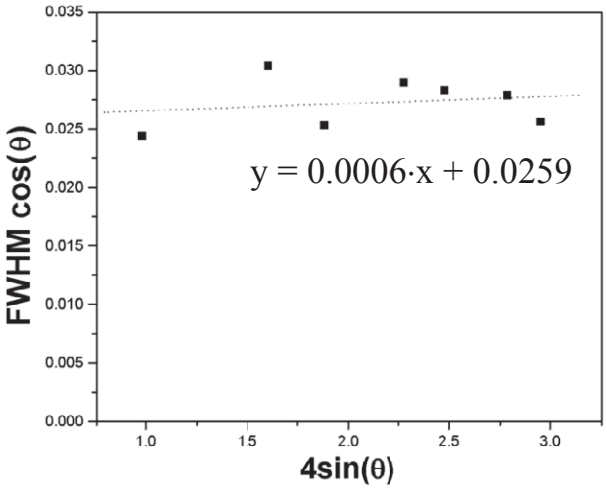

Figure S4. (top) XRD data for sample produced and annealed under the condition of 'sample A' (see Table 1), annealed at 800°C. The curve is fitted using Gaussian profiles for each crystalline peak and for the peaks due to the amorphous contribution. (bottom left) table with the crystalline peak position and their relative full width – half max (FWHM). (bottom right) Williamson-Hall plot: a linear fit of the data has negligible slope (proportional to stress acting on the crystal).

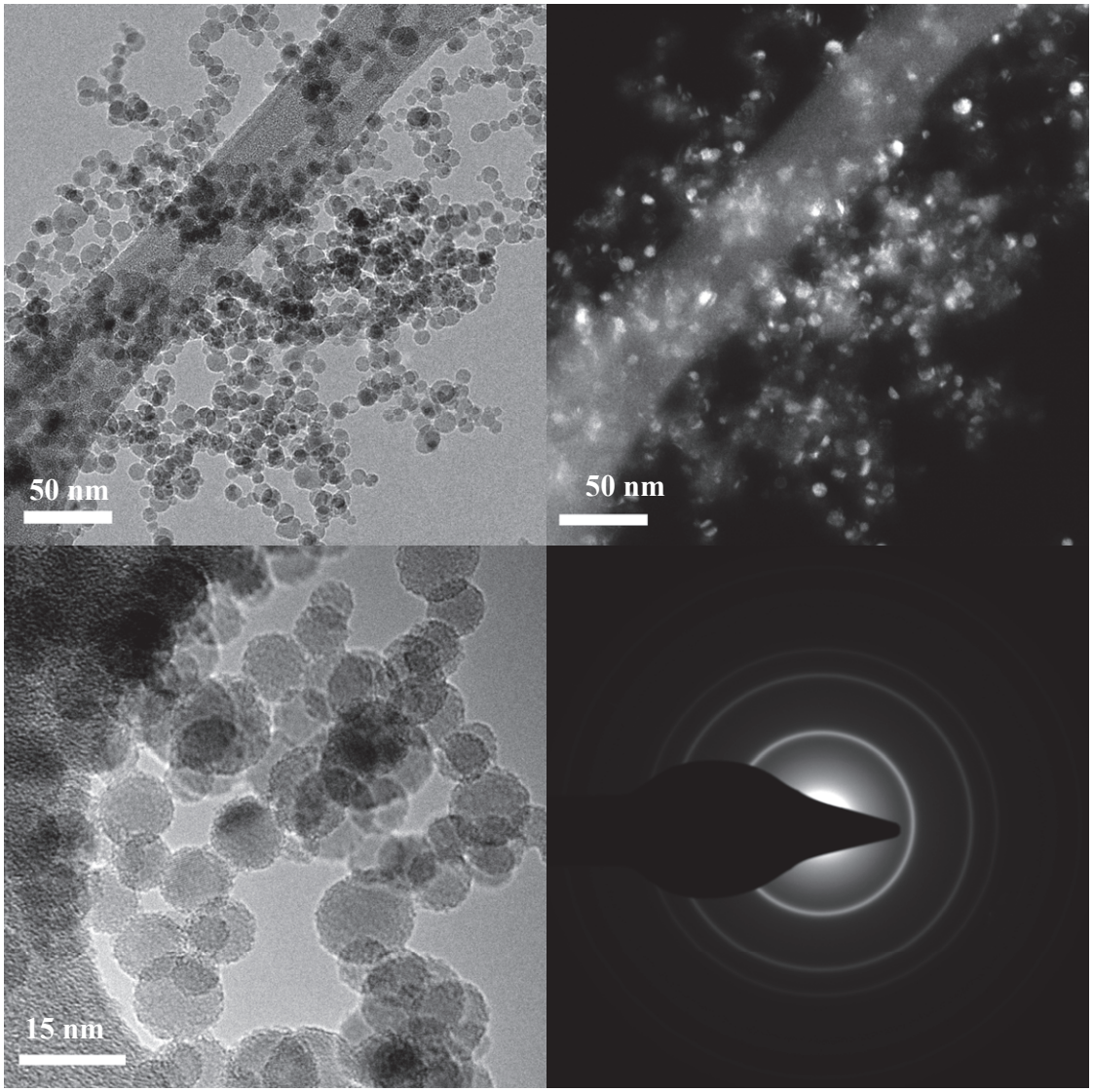

Figure S5. (a) Bright-field TEM micrograph of particles produced under the conditions of 'sample A' (see Table 1) and annealed at 830°C. (b) Dark field micrograph corresponding to (a). (c) Higher magnification micrographs, fringes from the [111] lattice planes are clearly visible. (d) Selected-area diffraction pattern generated using a low-magnification image, so that a large number of particles interact with the electron beam. Rings from the [111], [220] and [311] lattice planes are clearly distinguishable. These images support the conclusion that a very large fraction of the particles have a crystalline structure.

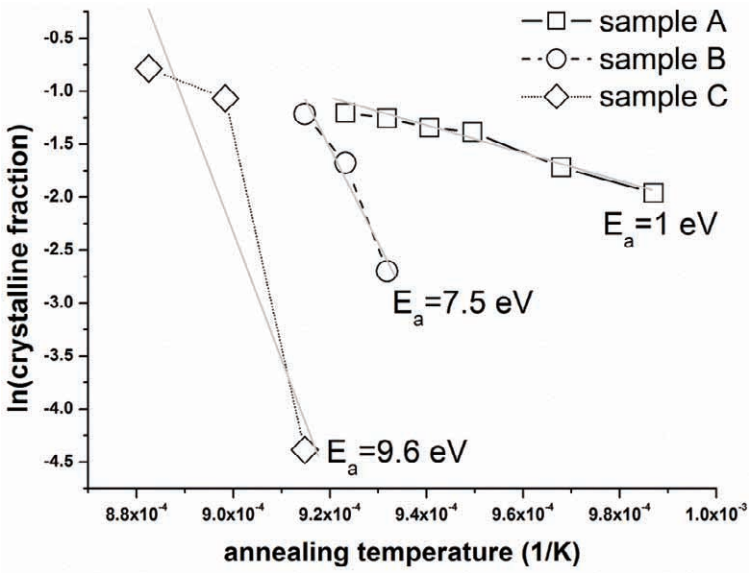

Figure S6. Arrhenius plot based on the data of figure 5. The activation energy for crystallization is 1 eV for the smaller particle size ranges (see table 1), and rapidly increases to 7.5 eV and 9.6 eV for increasingly larger sizes.

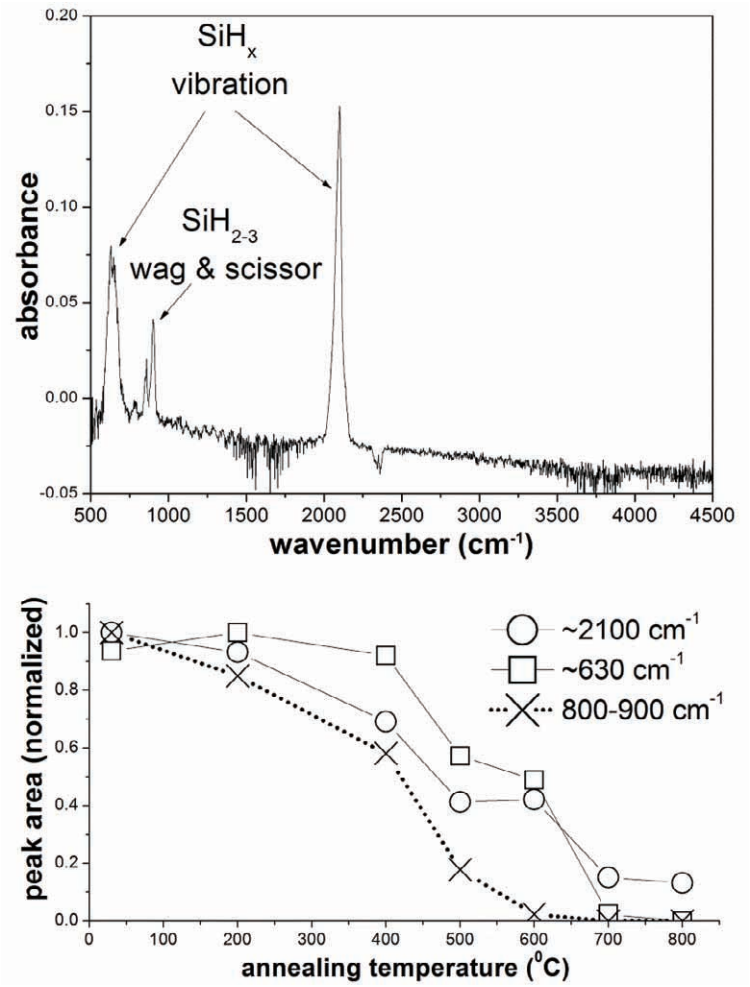

Figure S7. (top) FTIR absorbance from the plasma produced silicon nanoparticles, produced under the conditions of 'sample A' (see table 1) and without any in-flight annealing, as measured *in-situ* before air exposure. (bottom) Variation of the area under the ~2100 cm^{-1} peak, the ~630 cm^{-1} peak and the 800-900 cm^{-1}peaks with respect of the in-flight annealing temperature. The ~2100 cm^{-1} and the ~630 cm^{-1} peaks arise from SiH_x vibrational modes (x=1,2,3) while the 800-900 cm^{-1} peaks arise from SiH_2 and SiH_3 wag and scissor mode. Signal from the 800-900 cm^{-1} peaks diminishes faster than the signal from the ~2100 cm^{-1} and the ~630 cm^{-1} peaks, because of the lower thermal stability of higher surface hydrides.